Analysis of Fuel Ethanol Plant Liquor with the Composition Explicit Distillation Curve Method

Thomas J. Bruno,* Arron Wolk, and Alexander Naydich

Thermophysical Properties Division National Institute of Standards and Technology Boulder, Colorado

Received January 27, 2009. Revised Manuscript Received March 25, 2009

Although the use of ethanol and ethanol blends as motor fuels dates back to the earliest vehicles, ethanol has recently received extraordinary attention as a renewable liquid fuel. In the United States, the application of this fluid is mainly as an additive used to lower emissions (carbon monoxide and ozone), enhance antiknock index, and to extend gasoline stock. Elsewhere, such as in Brazil, mandated use raises ethanol to the level of a primary motor fuel. A major barrier to increased application of ethanol is the cost relative to gasoline, something that can be addressed to some extent by processing improvements, especially the distillation steps. Such improvements are not possible without the infrastructure of sound thermophysical property measurements, especially the distillation curves of the major plant streams. In this paper, we present the results of measurements made with the advanced distillation curve technique applied to five different process streams of a Brazilian ethanol plant. The advanced distillation curve method was recently introduced, and features: (1) a composition explicit data channel for each distillate fraction (for both qualitative and quantitative analysis); (2) temperature measurements that are true thermodynamic state points that can be modeled with an equation of state; (3) temperature, volume, and pressure measurements of low uncertainty suitable for equation of state development; (4) consistency with a century of historical data; (5) an assessment of the energy content of each distillate fraction; (6) trace chemical analysis of each distillate fraction; and (7) corrosivity assessment of each distillate fraction. We note that the head product from the stripping column is nearly identical to the residual flow from the molecular sieve columns, as is optimal since both streams are routed to the rectifier column. The head product from the rectifier column is a constant boiling azeotrope of ethanol and water, and the tail product from the rectifier column is nearly pure water.

Introduction

Fuel Ethanol. Fuel ethanol is usually made by the fermentation of simple sugars, followed by the distillation of the fermentation product, much the same way as potable alcoholic beverages are made. The main use of fuel ethanol in the United States has been as an additive for gasoline. It has been used as an oxygenate, to lower carbon monoxide emissions, and to improve antiknock properties (an octane booster).[1−4] Ethanol has also been suggested as an additive for diesel fuel.[5] The Clean Air Act Amendments of 1990 increased the usage of ethanol, since these acts required production of reformulated gasolines that mandated oxygenates.[6] This has been largely superseded by the Energy Policy Act of 2005, which established a renewable fuels standard (RFS). This mandates the addition of ethanol as a renewable extender in gasoline.[7−9]

In the United States, most fuel ethanol is made from corn, 75% of which is processed by dry milling, the remainder by a chemical process called wet milling.[3,10] Outside the United States, the largest producer and user of fuel ethanol is Brazil, where the primary feedstock is cane sugar.[11,12] There is an inherent difference in the processing economics as a consequence of the feedstock. The use of cane sugar results in the byproduct waste called bagasse, the fibrous residue remaining after sugar extraction. The bagasse is usually used as a fuel for plant steam production, and this steam is used to power the distillation steps. Moreover, excess energy that might be available from this step is used for cogeneration.

The large scale production of fuel ethanol in Brazil came about.[13] This effort, begun in response to the first oil crisis in 1975, was meant not only to produce a fuel but also to stabilize

* Author to whom correspondence should be addressed. E-mail: bruno@boulder.nist.gov.

(1) Wang, M.; Saricks, C.; Wu, M. *Fuel-cycle Fossil Energy Use and Greenhouse Gas Emissions of Fuel Ethanol Produced from U.S. Midwest corn, Report for the Illinois Department of Commerce*; Center for Transportation Research, Argonne National Laboratory: **1997**.

(2) Niven, R. K. *Renewable Sustainable Energy Rev.* **2005**, *9*, 535–555.

(3) Yaccobucci, B. D. *Fuel Ethanol: Background and Public Policy Issues, CRS Report for Congress, RL33290*; Congressional Research Service: Washington, D.C., March 3, 2006.

(4) Bonnema, G.; Guse, G.; Senecal, N.; Gupta, R.; Jones, B.; Ready, K. L. *Use of Midrange Ethanol/Gasoline Blends in Unmodified Passenger Cars and Light Duty Trucks* 1999Final Report - http://ethanol.org.

(5) Hansen, A. C.; Zhang, Q.; Lyne, P. W. L. *Bioresour. Technol.* **2005**, *96*, 277–285.

(6) Yaccobucci, B. D. *Alternative Fuels and Advanced Technology Vehicles: Issues in Congress, CRS Issue Brief for Congress, IB10125*; Congressional Research Service: Washington, D.C., May 8, 2008.

(7) Keefe, R.; Griffin, J. P.; Graham, J. D. *Risk Analysis* **2008**, *28* (5), 1141–1154.

(8) Yaccobucci, B. D. *Biofuels Incentives: A Summary of Federal Programs, CRS Report for Congress RL33572*; Congressional Research Service: Washington, D.C., July 25, 2006.

(9) Yaccobucci, B. D. *Ethanol Imports and the Caribbean Basin Initiative, CRS Report for Congress, RS21930*; Congressional Research Service: Washington, D.C., March 18, 2008.

(10) Arnold, F. H. *Eng. Sci.* **2008**, *71* (2), 12–19.

(11) Upadhiya, U. C. Production of ethanol from sugarcane. In Iberia Sugar TEC-254; Iberia Sugar: New Iberia, LA, 1996.

(12) Buchanan, E. J. *Sugar J.* **2002**, *65* (6), 11–17.

(13) Soccol, C. R.; Vandenburgehe, L. P. S.; Costa, B.; Woiciechoski, A. L.; Carvalho, J. C.; Medeiros, A. B. P.; Francisco, A. M.; Bonomi, L. J. *J. Sci. Ind. Res.* **2005**, *64* (11), 897–904.

10.1021/ef900077t
Published on Web 04/16/2009

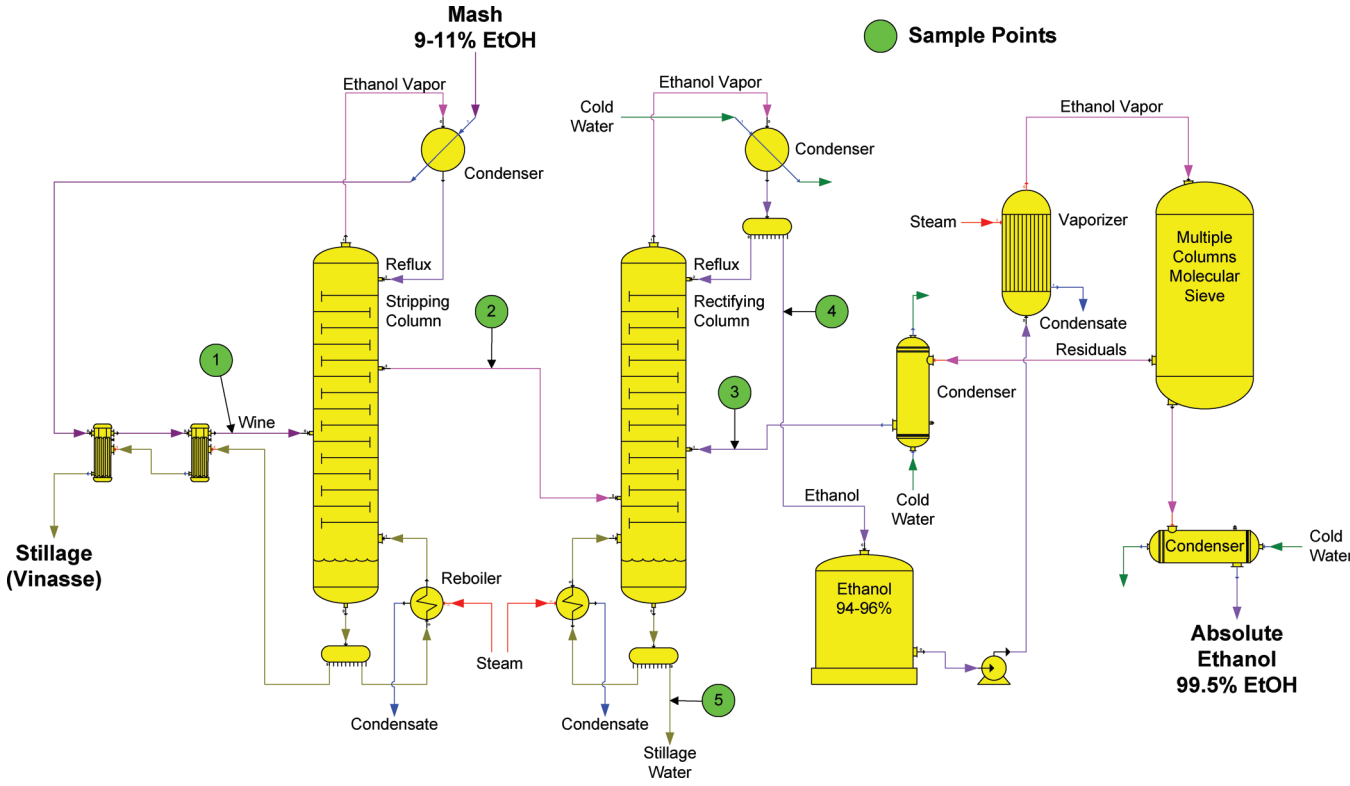

Figure 1. A flow diagram showing the essential features of the ethanol plant from which the samples measured in this work were taken. The sample points at which fluid was withdrawn for the measurement of distillation curves are indicated, Nos. 1−5.

sugar markets in that country. Before this, alcohol had been used as a fuel not only in Brazil but also worldwide, but on a much smaller scale.

The current supply of fuel ethanol in the United States comes not only from domestic production, but also from importation. The importation of ethanol has been facilitated in recent years by the Caribbean Basin Initiative (CBI), which has allowed duty-free importation of ethanol provided at least 50% of the product was produced by CBI beneficiary countries.[9] The provisions of this initiative have allowed a further 50% to come from other sources, when shipped from CBI beneficiary countries. It is clear from these factors that ethanol production from sources other than domestic corn is important to blending stocks in the United States.

Regardless of the feedstock or initial production steps (milling and fermentation, for example), the distillation of ethanol from alcoholic mash is a necessary and energy-intensive process.[14] Optimizing this step in the processing is important if ethanol is to be supplied without disruption, and if the use of ethanol is to compete economically in the absence of current significant subsidies.[15] One approach that is very promising and has been successfully applied on a relatively small scale is the operation of the distillation columns at slightly elevated pressures.[16] In addition, sets of successive columns can be operated at different pressures, primarily to produce a temperature difference between them. Then, one can use the top vapor of a higher pressure column to heat a column operated at a lower pressure. Overall, a plant operated in this way will use less steam than a plant with columns operated at ambient pressure, and in the case of the integrated sugar cane factory and distillery, more electrical power can be produced for export to the grid. The successful design of such plants is dependent upon adequate simulator models, which are in turn dependent on adequate thermophysical property inputs.

In this paper, we have applied a technique called the advanced distillation curve method to study the product fluids from five locations (sample points) of a modern ethanol plant, operating in Brazil, processing alcoholic mash produced from sugar cane. The overall flow diagram for this plant is provided in Figure 1. The locations at which samples have been drawn for this work are shown in Figure in the inset circles, labeled 1 through 5. More details about the samples are provided below. In this plant, the first and second distillation columns (noted as stripping and rectification) operate at a slight pressure difference (69 and 55 kPa, respectively). The second distillation column produces the azeotropic concentration of ethanol in water, typically 94% ethanol (mass/mass). In the past, further dehydration to fuel ethanol was done with the addition of benzene or cyclohexane to break the azeotrope, and subsequent distillation. More modern plants use a molecular sieve dehydration step, since this results in a lower energy consumption.[16] Although only one molecular sieve unit is shown in Figure 1, multiple units operate so that regeneration can be done without taking the entire plant off-line.

The Advanced Distillation Curve Approach. In earlier work, we described a method and apparatus for an advanced distillation curve (ADC) measurement that is especially applicable to the characterization of fuels.[17−22] This method is a significant improvement over current approaches, featuring (1) a composition explicit data channel for each distillate fraction (for both qualitative and quantitative analysis); (2) temperature measurements that are true thermodynamic state points that can be modeled with an equation of state; (3) temperature, volume, and pressure measurements of low uncertainty suitable for

(14) Wang, M.; Saricks, C.; Wu, M. *Fuel-cycle Fossil Energy Use and Greenhouse Gas Emissions of Fuel Ethanol Produced from U.S. Midwest Corn, Report for the Illinois Department of Commerce*; Center for Transportation Research, Argonne national Laboratory: **1997**.

(15) Satyro, M. A. *Material and Energy Balances for an Industrial Ethanol Plant, Internal Report*; Hyprotech Ltd.: Calgary, Canada, 1992.

(16) Seemann, F. *Int. Sugar J* **2003**, *105* (1257), 421–423.

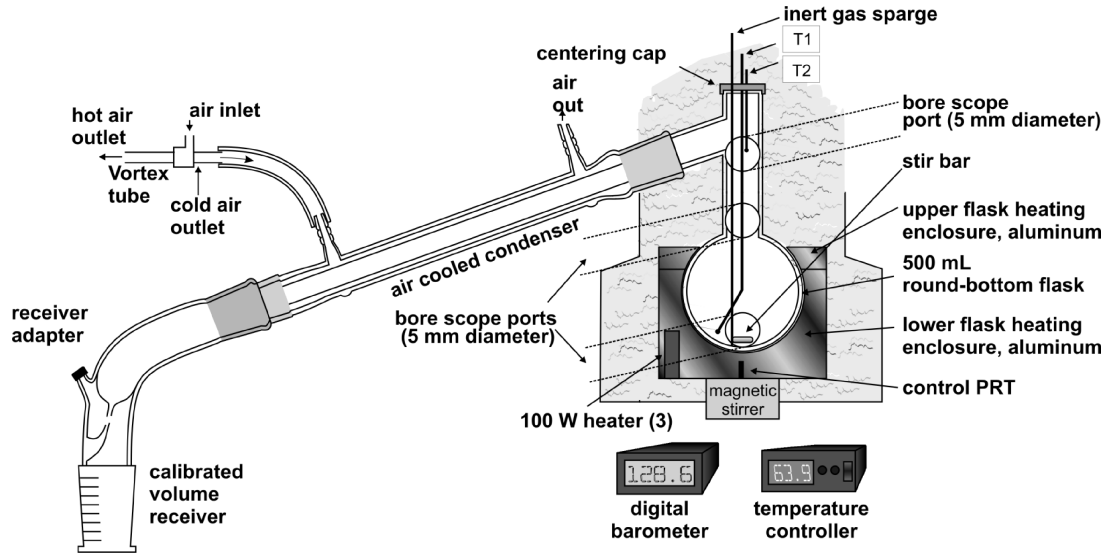

Figure 2. A schematic of the basic apparatus of the advanced distillation curve. Additional details can be found in references cited in the text.

equation of state development; (4) consistency with a century of historical data; (5) an assessment of the energy content of each distillate fraction; (6) trace chemical analysis of each distillate fraction; and (7) corrosivity assessment of each distillate fraction. The fuels we have measured include rocket propellants, gasolines, jet fuels, diesel fuels (including oxygenated diesel fuel and biodiesel fuels), and crude oils.[23−33]

The ADC apparatus consists of a stirred boiling flask that is placed in an aluminum enclosure that is itself very well insulated. Observation of the fluid inside the flask is done through small observations ports or a flexible bore scope, to optimize temperature uniformity. The fluid temperature is measured with thermocouples in two locations. One thermocouple monitors the temperature directly in the fluid (kettle) [T_k]. Another thermocouple is placed at the bottom of the takeoff position in the distillation head (T_h). Heat is applied to the enclosure (and ultimately to the kettle) with a model predictive controller. This is a temperature programmer that mimics the shape of a distillation curve but leads the temperature of the fluid in the flask by approximately 20 °C. This produces a constant mass flow rate of vapor through the distillation head. Following the distillation head, the vapor is condensed in a straight glass condenser chilled with air from a vortex tube. An adapter that allows for instantaneous sampling of the distillate follows the condenser, after which the distillate drops into a level stabilized receiver. A schematic diagram of the basic apparatus is provided in Figure 2.

In nearly all of our prior work on the ADC, we have presented the thermodynamic state point data as the temperature measured directly in the fluid (T_k). This has been demonstrated numerous times to be the correct approach, by making measurements on mixtures of known compositions. In the measurements of mixtures in which water makes up a significant fraction, we have found that this approach does not work. This is due to the very high heat capacity of water, which causes strikingly different behavior when this fluid is boiled. Any fluid will proceed through four distinct regimes when being heated to boiling, although the differences are especially pronounced with water. As water is heated to boiling (in the absence of agitation), one first notes the appearance of small bubbles of dissolved gas that pinch off the container surface and rise, usually to be coalesced into the bulk.[34] This is termed the isolated vapor bubble regime. As heating is continued, columns of vapor form at the surface of the enclosure and rise to the surface in a regime called nucleate boiling. If the temperature of the surroundings is raised further, the surface of the enclosure becomes covered with a layer of vapor that will slow the transfer of heat. This is the transition regime. If the enclosure temperature is further raised, eventually the entire surface will be covered with vapor. This is called the film boiling regime.

In our previous experiments with aqueous mixtures, we noted that when heating rates comparable to those used for hydrocarbons were used, the distillations became very slow and sometimes would not be complete even after 120 min. This was striking when starting with 200 mL of an aqueous mixture, even after the enclosure temperature was raised to very high levels, sometimes approaching 400 °C. In contrast, in the measurement of a hydrocarbon-based fluid such as diesel fuel, the distillations would be complete in approximately 40 min, and the enclosure temperature would lead the fluid temperature by 20 °C. Moreover, we noted with aqueous mixtures that the temperature T_k indicated significant superheating, and was therefore not useful as thermodynamic state points of the mixture. Under these

(17) Bruno, T. J. *Ind. Eng. Chem. Res.* **2006**, *45*, 4371–4380.
(18) Bruno, T. J.; Smith, B. L. *Ind. Eng. Chem. Res.* **2006**, *45*, 4381–4388.
(19) Bruno, T. J. *Sep. Sci. Technol.* **2006**, *41* (2), 309–314.
(20) Smith, B. L.; Bruno, T. J. *Int. J. Thermophys* **2006**, *27*, 1419–1434.
(21) Bruno, T. J.; Smith, B. L. *Energy Fuels* **2006**, *20*, 2109–2116.
(22) Ott, L. S.; Smith, B. L.; Bruno, T. J. *J. Chem. Thermodynam.* **2008**, *40*, 1352–1357.
(23) Smith, B. L.; Bruno, T. J. *Ind. Eng. Chem. Res.* **2007**, *46*, 297–309.
(24) Smith, B. L.; Bruno, T. J. *Ind. Eng. Chem. Res.* **2007**, *46*, 310–320.
(25) Ott, L. S.; Smith, B. L.; Bruno, T. J. *Fuel* **2008**, *87*, 3055–3064.
(26) Ott, L. S.; Smith, B. L.; Bruno, T. J. *Fuel* **2008**, *87*, 3379–3387.
(27) Ott, L. S.; Smith, B. L.; Bruno, T. J. *Energy Fuels* **2008**, *22*, 2518–2526.
(28) Smith, B. L.; Ott, L. S.; Bruno, T. J. *Environ. Sci. Technol.* **2008**, *42* (20), 7682–7689.
(29) Ott, L. S., Hadler, A., Bruno, T. J. *Eng. Chem. Res.* **2008**, *47* (23), 9225−9233.
(30) Ott, L. S.; Bruno, T. J. *Energy Fuels* **2008**, *22*, 2861–2868.
(31) Smith, B. L.; Bruno, T. J. *Energy Fuels* **2007**, *21*, 2853–2862.
(32) Smith, B. L.; Bruno, T. J. *J. Propul. Power* **2008**, *24* (3), 619–623.
(33) Smith, B. L.; Ott, L. S.; Bruno, T. J. *Eng. Chem. Res.* **2008**, *47* (16), 5832–5840.
(34) Halliday, D.; Resnick, R.; Walker, J. Boiling and the Leidenfrost Effect. In *Fundamentals of Physics*, 4th ed.; John Wiley and Sons: New York, 1993.

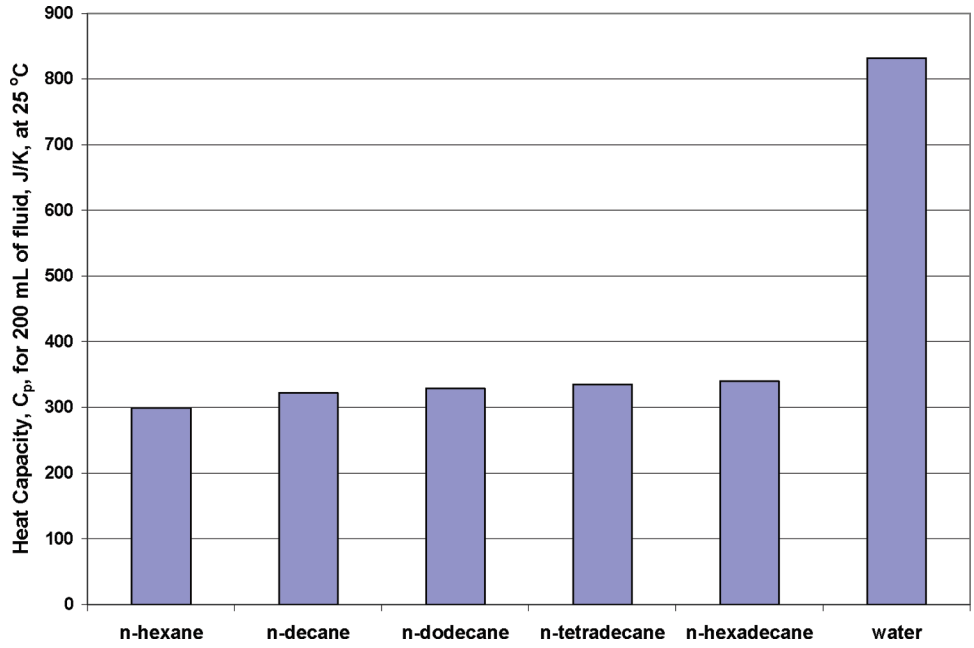

Figure 3. A histogram showing the magnitude of the heat capacity, C_p, of selected n-alkanes and water, calculated for 200 mL of fluid at 25 °C. The uncertainty of each value is estimated to be less than 1%.

Table 1. Representative Distillation Curve Data for a Prepared Mixture of Ethanol and Water, 50/50 vol/vol[a]

distillate volume fraction, %	T_h, °C (83.0 kPa)
5	81.9
10	82.0
15	82.7
20	83.0
25	83.6
30	84.6
35	85.1
40	85.7
45	86.4
50	87.6
55	90.8
60	94.1
65	98.3
70	99.9
75	100.0
80	100.0
85	100.0
90	100.0

[a] The temperatures in this table have been adjusted with the Sydney Young equation to what would be obtained at atmospheric pressure. The experimental pressures are provided in parentheses to allow recovery of the actual experimental temperatures. The uncertainties are discussed in the text.

circumstances, we noted that the temperature in the head, T_h, located away from the pronounced transition regime in the kettle, was providing the correct thermodynamic state point. It is unlikely that we ever entered the film boiling regime with the ADC apparatus.

The reason that the behavior described above occurred with water mixtures, but not with hydrocarbon mixtures, is due to the much higher heat capacity of water. This can be demonstrated in Figure 3, a histogram showing the C_p of several n-alkanes (representative of the fuels we have measured previously), along with water.[35] The heat capacity we have presented here is calculated at 25 °C, for 200 mL of fluid (to mimic how an ADC measurement is done). The significantly higher C_p for this volume of fluid is the cause of the pronounced transition boiling regime encountered with aqueous mixtures; a situation not encountered with the hydrocarbon fluids.

(35) Rowley, R. L.; Wilding, W. V.; Oscarson, J. L. ; Zundel, N. A.; Marshall, T. L.; Daubert, T. E.; Danner, R. P. *DIPPR Data Compilation of Pure Compound Properties*; Design Institute for Physical Properties: New York, 2004.

Table 2. The Initial Boiling Temperatures (Presented As the Vapor Rise Temperature in T_h) of the Five for Five Samples from an Ethanol Distillation Plant[a]

sample, location, pressure	observed temperatures, T_h, °C
wine 1 (83.39 kPa)	80.1
stripping to rectification 2 (83.63 kPa)	78.9
residue from dehydration 3 (83.74 kPa)	79.2
rectification to dehydration 4 (83.26 kPa)	79.6
tail from rectification 5 (83.46 kPa)	100.3

[a] The sample locations with the column headings correspond to those on the process flow sheet, Figure 1. The temperatures in this table have been adjusted with the Sydney Young equation to what would be obtained at atmospheric pressure. The experimental pressures are provided in parentheses to allow recovery of the actual experimental temperatures. The uncertainties are discussed in the text.

Experimental Section

The fluids taken from the specified sample points in Figure 1 were obtained from a collaborative fuel ethanol distillery in Brazil. The samples were provided in sealed, opaque containers to prevent the escape of volatile constituents. Since some of the samples had a sediment settle out to the bottom of the containers, samples were prepared by centrifugation at 3500 rpm for 1 h in sealed polyethylene centrifuge tubes. Only the supernatant liquid was used for measurement. No additional steps were taken to prepare the samples. All of the samples had an odor, some very distinctive. In the case of the "wine", the solid precipitate was plant matter, whereas that present in later samples was black or gray, indicative of scale. The feedstock sample from location 1, labeled "wine", had a distinct odor of molasses. This fluid typically consists of an aqueous solution of 6.5% (mass/mass) ethanol, and is a dark reddish brown in color. Sample 2 was the head product from the stripping column, a clear fluid with a slight odor resembling dilute table wine. Sample 4 was the head product from the rectification column, also clear with the same slight odor as the head product from sample point 2. Sample 3 is the underflow or residual flow that results from the reactivation of the molecular sieve columns. With one molecular sieve column in service dehydrating the azeotrope, others

Table 3. Representative Distillation Curve Data for Five Samples from an Ethanol Distillation Plant[a]

	T_h, °C				
distillate volume fraction, %	wine (83.39 kPa), **1**	stripping to rectification (83.63 kPa), **2**	residue from dehydration (83.74 kPa), **3**	rectification to dehydration (83.26 kPa), **4**	tail from rectification (83.46 kPa), **5**
5	93.7	81.3	80.7	78.9	100.5
10	96.3	81.5	81.0	79.0	100.5
15	97.6	81.8	81.1	79.0	100.5
20	99.2	82.2	81.4	79.0	100.4
25	99.7	82.6	81.7	78.9	100.4
30	99.8	82.9	81.7	79.0	100.4
35	99.9	83.2	82.2	79.0	100.5
40	99.9	83.9	82.6	78.9	100.4
45	99.9	84.9	83.6	78.9	100.5
50	100.0	85.5	85.3	78.9	100.4
55	99.9	87.7	87.6	79.1	100.5
60	99.9	91.0	90.8	79.0	100.4
65	99.9	96.3	95.5	79.0	100.5
70	99.9	100.1	99.3	79.1	100.3
75	100.1	100.0	100.0	79.0	100.5
80	100.0	100.0	99.9	79.0	100.6
85	100.0	100.0	99.9	79.0	100.5
90	100.0	100.0	99.9	79.0	100.4

[a] The sample locations with the column headings correspond to those on the process flow sheet, Figure 1. The temperatures in this table have been adjusted with the Sydney Young equation to what would be obtained at atmospheric pressure. The experimental pressures are provided in parentheses to allow recovery of the actual experimental temperatures. The uncertainties are discussed in the text.

are being recycled, and the carryover is sent to the rectifier to avoid loss of the ethanol it contains. Ideally, the plant is operated such that the two inputs to the rectifying column are comparable in composition and volatility. This corresponds to samples 2 and 3 in Figure 1. Sample 5 is the tail product from the rectification column (also called lutter water). It consists of nearly pure water, but it too has a characteristic odor of very dilute table wine. The lutter water can be returned for use elsewhere in the plant, used for irrigation or disposed of in a sewer. There are environmental consequences for the disposal of lutter water since it can sometimes have a relatively high biological oxygen demand (BOD). We note that the same environmental issue pertains to the vinasse, the tail product from the stripping column shown in Figure 1.

The solvent used to dilute the analytical samples taken in the course of the measurements on these samples was n-butanol, chosen to provide no chromatographic interference from the analytical components of interest: ethanol and water. The n-butanol was dried over molecular sieves. The purity of the n-butanol was verified with gas chromatography with mass spectrometry and flame ionization detection (30 m capillary column of 5% phenyl−95% dimethyl polysiloxane having a thickness of 1 μm, temperature program from 90 to 170 at 7 °C per minute). Calibrations for ethanol were performed with the external standard method, a calibration curve being prepared from five solutions of ethanol in n-butanol. Analyses were then done by gas chromatography with flame ionization detection.

Water analysis was performed with Karl Fisher coulombic titrimetry. These analyses demonstrated that the solvent was of sufficient purity (99.9%, mass/mass) for our application. The Karl Fisher instrument was calibrated with commercial calibration solutions before use. The uncertainty in the water determination was 10 ppm (mass/mass). Refractive index measurements were done with an Abbe-type refractometer that was thermostatted with a circulating bath to 25 °C. The uncertainty in temperature was 0.1 °C, and the uncertainty in the refractive index was 0.0005.

The method and apparatus for the distillation curve measurement has been reviewed in a number of sources, so additional general description will not be provided here. The required fluid for the distillation curve measurement (in each case 200 mL) was placed into the boiling flask with a 200 mL volumetric pipet. The thermocouples were then inserted into the proper locations to monitor T_k—the temperature in the fluid—and T_h—the temperature at the bottom of the takeoff position in the distillation head. Enclosure heating was then commenced with a four-step program based upon a previously measured distillation curve. Volume measurements were made in the level-stabilized receiver, and 7 μL sample aliquots were collected at the receiver adapter hammock. Samples withdrawn for the chromatographic determination of ethanol were dissolved in n-butanol as a solvent, and samples used for water analysis and refractive index measurement were collected without solvent. In the course of this work, we performed between four and six complete distillation curve measurements for each of the five fluid samples.

Since the measurements of the distillation curves were performed at ambient atmospheric pressure (approximately 83 kPa, measured with an electronic barometer), temperature readings were corrected for what should be obtained at standard atmospheric pressure. This was done with the modified Sidney Young equation, in which the constant term was assigned a value of 0.000 096 5. The raw temperatures measured in our laboratory (located at an elevation of 1655 m) can be recovered from the Sydney Young equation.

Results and Discussion

The feed fluid (the wine) from the cane sugar fermentation process will undoubtedly have some variability, depending on the weather conditions during the growing season and also the fermentation treatment. Indeed, over the course of a growing season, the processing plant from which the samples were obtained observes a variation of 8.4% in ethanol concentration in this feed fluid, although the typical ethanol concentration is 6.5% (mass/mass).[36] This level of variability is not surprising, thus the wine measured here might not be representative of all crop conditions. The samples from locations 2−5, however, are typical and representative of the plant conditions. These samples are not expected to vary by more than 1−2% in either compositions or volatility.

Before presenting the measurements on the plant samples, we first present representative data on a prepared mixture of ethanol and water, 50/50 vol/vol, in Table 1. These data have been adjusted with the Sydney Young equation, and the experimental pressure is provided so that the raw experimental temperature can be recovered if desired. These data demonstrate that the apparatus is functioning properly and that T_h is providing the thermodynamic state point of the mixture.

Initial Boiling Temperatures. During the initial heating of each sample in the distillation flask, the behavior of the fluid was carefully observed. Direct observation through the flask

(36) Weiss, W. Sugars International: Englewood, CO, 2008; personal communication.

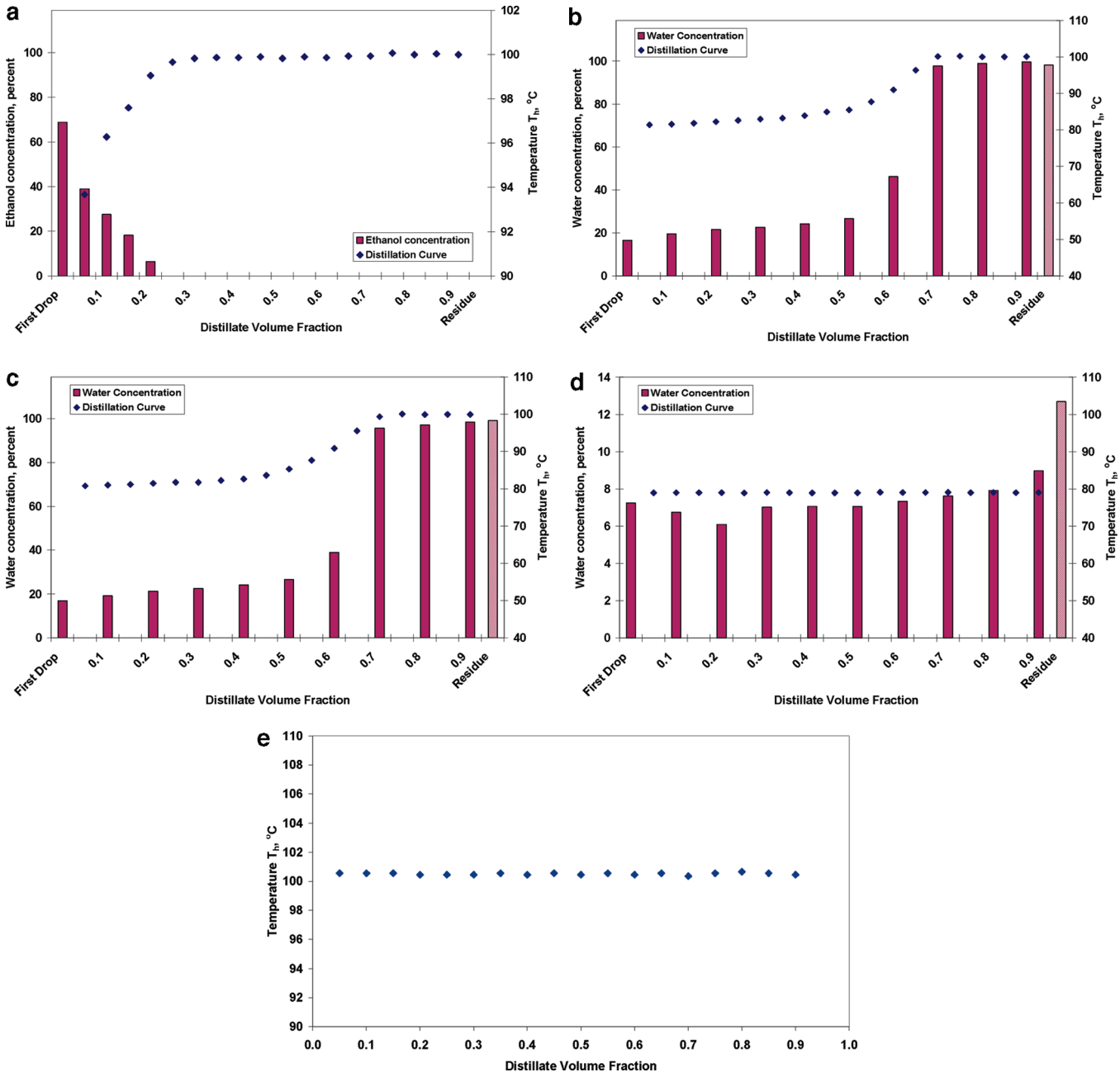

Figure 4. (a) A representative distillation curve, presented as T_h, of the wine sample taken at position 1 in Figure 1. Also presented is the measured ethanol concentration (mass/mass). (b) A representative distillation curve, presented as T_h, of the sample from the stripping column as it enters the rectification column (position 2 in Figure 1). Also presented is the measured water concentration (mass/mass). (c) A representative distillation curve, presented as T_h, of the sample of the residue from the molecular sieve dehydration, passed back to the rectification column (position 3 in Figure 1). Also presented is the measured water concentration (mass/mass). (d) A representative distillation curve, presented as T_h, of the sample from the rectification column (position 4 in Figure 1). Also presented is the measured water concentration (mass/mass). (e) A representative distillation curve, presented as T_h, of the sample of the tail product from the rectification column, or the lutter water (position 5 in Figure 1).

window or through the bore scope allowed measurement of the onset of boiling for each of the mixtures. Typically, the first bubbles will appear intermittently and will quell if the stirrer is stopped momentarily. Sustained vapor bubbling is then observed. In the context of the advanced distillation curve measurement, sustained bubbling is also somewhat intermittent, but it is observable even with the stirrer is momentarily stopped. Finally, the temperature at which vapor is first observed to rise into the distillation head is observed. This temperature is termed the vapor rise temperature, which we have shown is actually the initial boiling temperature of the mixture. These observations are important because they can be modeled theoretically, for example, with an equation of state. The uncertainty in the vapor rise temperature is 0.3 °C (determined from previous studies on well-defined fluids). In the case of these aqueous mixtures, in which superheating occurs in the temperature measured with T_k, we present only the vapor rise temperature measured as T_h. These data are presented in Table 2 for each of the five ethanol plant samples. We note that for samples 1−4 the initial boiling temperatures are remarkably consistent. Moreover, the measured temperatures are consistent with mixtures of ethanol and water, with evidence of other trace components from the fermentation. The temperatures are slightly higher than what would be expected for a mixture of only ethanol and water. For sample 5, the lutter water, we note that the initial boiling temperature is

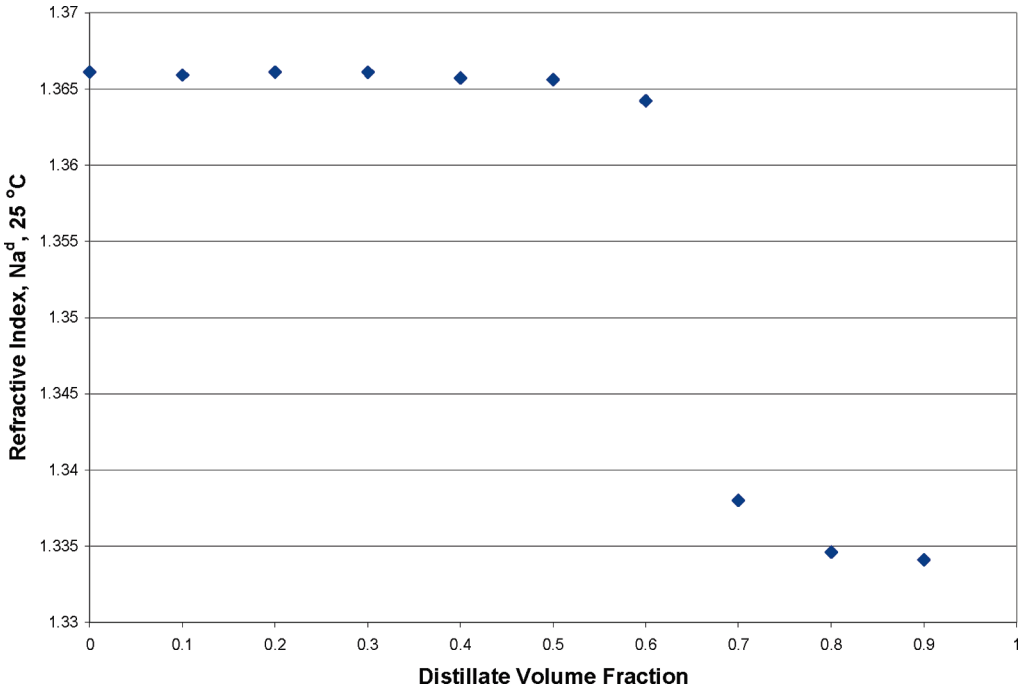

Figure 5. A plot of the refractive index as a function of distillate fraction for the head product from the stripping column before being sent to the rectification column (sample point 2).

indicative of nearly pure water with no ethanol, although trace impurities are again present.

Distillation Curves and Compositional Information. Representative distillation curve data measured with the ADC instrument are presented in Table 3. These data are presented in terms of T_h, the temperature measured at the bottom of the take-off position in the distillation head, as discussed above. Because there are no meaningful T_k data due to superheating in this aqueous mixture, we are not able to observe the difference or convergence that indicates the presence of azeotropy. The T_h data for these samples are instructive nonetheless. We note that the distillation temperatures of the wine begin at a temperature indicative of the presence of ethanol (approximately 94 °C); by the 20% distillate fraction this is now essentially water. The sample from the stripping column and the residue from the dehydration column appear to be very similar in their behavior. These mixtures start with a temperature slightly above that of the ethanol + water azeotrope (78.1 °C at a concentration of 96% ethanol, mass/mass), and proceed to the boiling temperature of pure water by the 70% distillate fraction. The sample from the rectifying column boils at a constant temperature that is consistent with the azeotropic concentration of ethanol + water over the entire range. We note that the boiling temperature is slightly higher than the reported mixture boiling temperature, likely because of the presence of other trace constituents. The distillation data for the rectifier tail (the lutter water) is indicative of nearly pure water, but again the temperature is slightly elevated. We note that with the pure ethanol + water mixture, no such increase was observed. The slight elevation in temperature is, however, consistent with observance of a slight odor to the lutter water. Clearly, there were trace quantities of other constituents present.

The distillation curves for these five samples are plotted in Figure 4, along with analytical information from the composition explicit data channel. For the wine feed stock fluid, we note that the first drop of distillate has an ethanol concentration of nearly 70% (mass/mass), and this concentration drops as the distillation proceeds. At the same time, the distillation temperature increases as the ethanol is removed. We no longer observe any ethanol in the distillate by the 0.25 distillate volume fraction. The corresponding temperature at this point is indicative of nearly pure water. The distillation begins at a higher temperature than the stripped or rectified product, indicative of the cruder feed stock.

The distillation curves and composition data for the inputs to the rectifying column will be discussed together. In Figures 4b and 4c, we plot the distillation curves along with the corresponding water concentration for the stripping column head product and the underflow (or residual flow) from reactivation of the molecular sieve columns. As we noted in the experimental section, it is desirable that these two streams be similar, since they both feed the rectification column. The distillation data of Table 3 for these two samples are very similar, and the curves with the water concentration bear this out; the two streams are nearly identical in volatility and composition. For both samples, the water content increases slightly until a distillate fraction of 0.5, at which point the concentration increases sharply. The temperature tracks the behavior of the composition of the distillate very well.

The distillation curve of the sample taken from the head of the rectification column (Figure 4d) is striking in that it is essentially flat at the azeotrope of ethanol and water, with the corresponding water concentration at the azeotropic mixture. This behavior persists until the very end of the distillation, at which point the water content increases to the residue. Finally, in Figure 4e we see the distillation curve for the tail product from the rectification column (the lutter water). This curve is also flat, corresponding to nearly pure water. The boiling temperature is slightly above that observed for pure water, however, consistent with the observation of an odor in this sample before and during the distillation curve measurement. There are trace constituents that slightly elevate the boiling temperature. This stream was analyzed for the presence of ethanol, and none was found in any fraction.

As an example of another analytical technique that can be applied to the ADC measurement, we present in Figure 5 the refractive index as a function of distillate fraction for the head product from the stripping column (sample point 2). Refractive

index, and the related Brix scale for sugar content, are often applied to process streams in sugar processing plants and distilleries. As an analytical technique, it is simple, inexpensive, and can be implemented with minimal training to personnel. We note that the refractive index corresponds precisely with the distillation curve and water content presented in Figure 4b. Refractive index is yet another analytical channel that can be routinely applied to the ADC approach.

Conclusions

In this paper we have presented an analysis of the major plant liquors in a operating, commercial fuel ethanol plant with the advanced distillation curve approach. This method allows complex fluids to be characterized and modeled with equations of state since the temperatures are thermodynamic state points.[37,38] The composition explicit data channel of the method allows the temperatures to be related to changing compositions. We note that the head product from the stripping column is nearly identical to the residual flow from the molecular sieve columns, as is optimal since both streams are routed to the rectifier column. The head product from the rectifier column is a constant boiling azeotrope of ethanol and water, and the tail product from the rectifier column is nearly pure water.

Acknowledgment. A.W. and A.N. acknowledge Summer Undergraduate Research Fellowships (SURF) at NIST. The authors acknowledge the assistance and collaboration of Warner Weiss of Sugars International LLC, Englewood, Colorado, USA, for providing the plant samples measured in this work.

EF900077T

(37) Huber, M. L.; Smith, B. L.; Ott, L. S.; Bruno, T. J. *Energy Fuels* **2008**, *22*, 1104–1114.

(38) Huber, M. L.; Lemmon, E.; Diky, V.; Smith, B. L.; Bruno, T. J. *Energy Fuels* **2008**, *22*, 3249–3257.